Nonlinear Dynamics of Slender Rods

A. Rosen,* R. G. Loewy,† and M. B. Mathew‡
Rensselaer Polytechnic Institute, Troy, New York

The nonlinear equations of motion of a rod undergoing small strains and moderate elastic rotations are derived. The derivation uses a variational approach and the equations of motion are obtained by applying Lagrange's equations. The results of a recently developed "principal curvature transformation" are employed to account for the structural aspects. Generalized coordinates are also used to establish an efficient analysis method. By a direct perturbation of the nonlinear equations of motion, the relations governing the small vibrations of a rod superimposed on finite static deformations are obtained. The theory is validated by comparing its results with experimental results available in the literature. Good agreement is obtained. In addition, the influences of nonlinear effects on such vibrations are pointed out and discussed.

Introduction

A NEW approach to the analysis of pretwisted rods subject to loads sufficient to cause large deflections has been developed.[1,2] In this case, the term "large deflections" implies nonlinear, coupled bending torsion behavior. The method is based on a principal curvature transformation and the use of generalized coordinates. The resulting theory has been checked by comparing results obtained through its application to the prediction of deflections under static transverse loads with available experimental results and other theoretical calculations for such cases. These investigations have shown that the new method is both accurate and efficient.

It is noted that the derivation in Refs. 1 and 2 deals only with static cases. The purpose of the present paper is to extend the static analysis of Refs. 1 and 2 to include dynamic cases as well. An expression for the kinetic energy of a rod undergoing relatively large displacements and moderately large rotations is first derived. Then, by using Lagrange's equations and the results of Refs. 1 and 2, the equations of motion of the rod are obtained. Perturbation techniques are then applied to yield the appropriate equations for small vibrations superimposed on finite deformations. As the final step, the validity of these equations is checked by comparing experimental results available in the literature for rods having zero pretwist with the results of this new theory.

The Kinetic Energy of a Deformed Rod

A Cartesian system of coordinates x, y, and z is used to describe the rod before and after deformation. In the undeformed state, the elastic axis of the rod coincides with the x coordinate line. The rod root is positioned at $x = 0$ and its tip at $x = L$. Each material point of the rod is characterized in terms of its coordinates (x, y, z) in the undeformed states and $\boldsymbol{e}_x$, $\boldsymbol{e}_y$, and $\boldsymbol{e}_z$ unit vectors in the directions of the coordinate lines x, y, and z, respectively.

The translational displacements of each point on the elastic axis are defined by the components u, v, and w in the directions $\boldsymbol{e}_x$, $\boldsymbol{e}_y$, and $\boldsymbol{e}_z$, respectively. In addition, there is a rotation of the cross section about its local elastic axis by an angle ϕ (for a more detailed discussion of elastic rotations, see Refs. 1 and 2). As a result of these deformations, the triad of unit vectors originally designated as $\boldsymbol{e}_x$, $\boldsymbol{e}_y$, $\boldsymbol{e}_z$ are rotated at a general point along the elastic axis away from the fixed Cartesian coordinates, x, y, z into a new set of orthogonal unit vectors: $\boldsymbol{e}_{x1}, \boldsymbol{e}_{y1}, \boldsymbol{e}_{z1}$. Using the results of Ref. 1 (Eq. A-9) and neglecting terms of fourth and higher orders (i.e., products of four displacements or their derivatives) yield the following expression for this transformation:

$$\boldsymbol{e}_{x1} = \left(1 - \underline{\tfrac{1}{2}v_{,x}^2} - \underline{\tfrac{1}{2}w_{,x}^2}\right)\boldsymbol{e}_x + v_{,x}\boldsymbol{e}_y + w_{,x}\boldsymbol{e}_z \tag{1a}$$

$$\boldsymbol{e}_{y1} = -\left(v_{,x} + \underline{\tfrac{1}{2}v_{,x}w_{,x}^2} + \phi w_{,x}\right)\boldsymbol{e}_x + \left(1 - \underline{\tfrac{1}{2}v_{,x}^2} - \underline{\phi v_{,x}w_{,x}}\right)\boldsymbol{e}_y + \phi\left(1 - \underline{\tfrac{1}{2}w_{,x}^2}\right)\boldsymbol{e}_z \tag{1b}$$

$$\boldsymbol{e}_{z1} = -\left(w_{,x} - \underline{\tfrac{1}{2}v_{,x}^2 w_{,x}} - v_{,x}\phi\right)\boldsymbol{e}_x - \left(\phi - \underline{\tfrac{1}{2}v_{,x}^2\phi} + v_{,x}w_{,x}\right)\boldsymbol{e}_y + \left(1 - \underline{\tfrac{1}{2}w_{,x}^2}\right)\boldsymbol{e}_z \tag{1c}$$

As might be expected (note that only the angle ϕ and derivatives of v and w are involved) and as will be shown later, this transformation influences only the contributions of the cross-sectional rotations to the kinetic energy. It is well known that these contributions are very small in the case of slender rods and that, in fact, their influence on transverse vibrations is usually negligible. Therefore, to minimize complications, the underlined terms in Eqs. (1) will be neglected when they contribute to cross-sectional rotations, but not when they contribute to translational displacements. This is equivalent to neglecting the products of elastic rotations compared with unity.

If the Bernoulli-Euler hypothesis is assumed to apply (for details, see Ref. 1), then the position vector of any point after deformation is given by

$$\bar{R} = (x + u)\boldsymbol{e}_x + v\boldsymbol{e}_y + w\boldsymbol{e}_z + y\boldsymbol{e}_{y1} + z\boldsymbol{e}_{z1} + \tilde{\psi}\boldsymbol{e}_{x1} \tag{2}$$

where $\tilde{\psi}$ is the warping displacement of the cross section, which is to be assumed small compared to v and w. Substitution of Eqs. (1b) and (1c) into Eq. (2) yields

$$\bar{R} = \left[x + u + \tilde{\psi} - y(v_{,x} + \phi w_{,x}) - z(w_{,x} - \phi v_{,x})\right]\boldsymbol{e}_x + \left[v + \tilde{\psi}v_{,x} + y - z(\phi + v_{,x}w_{,x})\right]\boldsymbol{e}_y + \left[w + \tilde{\psi}w_{,x} + y\phi + z\right]\boldsymbol{e}_z \tag{3}$$

Received Jan. 20, 1986; revision received July 25, 1986,

*Senior Post Doctoral Fellow (on sabbatical leave from Department of Aeronautical Engineering, Technion—Israel Institute of Technology, Haifa). Member AIAA.
†Institute Professor. Fellow AIAA.
‡Graduate Student.

The velocity of each material point at any moment is obtained by differentiating Eq. (3) with respect to time. Assuming that the contributions of warping to the velocities are very small and can be neglected, we obtain

$$\dot{\bar{R}} = \left[\dot{u} - y\left(\dot{v}_{,x} + \dot{\phi} w_{,x} + \phi \dot{w}_{,x}\right) - z\left(\dot{w}_{,x} - \dot{\phi} v_{,x} - \phi \dot{v}_{,x}\right)\right] \boldsymbol{e}_x + \left[\dot{v} - z\left(\dot{\phi} + \dot{v}_{,x} w_{,x} + v_{,x} \dot{w}_{,x}\right)\right] \boldsymbol{e}_y + \left[\dot{w} + y\dot{\phi}\right] \boldsymbol{e}_z \tag{4}$$

The total kinetic energy T is obtained by integrating over the whole rod volume; i.e.,

$$T = \frac{1}{2} \int_0^L \int\int_A \rho \left(\dot{\bar{R}} \cdot \dot{\bar{R}}\right) \mathrm{d}A \, \mathrm{d}x \tag{5}$$

where ρ is the mass density of the rod, which may be a function of x, y, or z, and A the rod cross section.

Substituting Eq. (4) into Eq. (5) and integrating over the cross-sectional area yields

$$\begin{aligned} T = \frac{1}{2} \int_0^L \{ & m\left(\dot{u}^2 + \dot{v}^2 + \dot{w}^2\right) \\ & + 2m\left[-y_{cg}\dot{u}\left(\dot{v}_{,x} + \dot{\phi} w_{,x} + \phi \dot{w}_{,x}\right)\right. \\ & - z_{cg}\dot{u}\left(\dot{w}_{,x} - \dot{\phi} v_{,x} - \phi \dot{v}_{,x}\right) - z_{cg}\dot{v}\left(\dot{\phi} + \dot{v}_{,x} w_{,x} + v_{,x} \dot{w}_{,x}\right) \\ & \left. + y_{cg}\dot{w}\dot{\phi}\right] + MI_{yy}\left(\dot{v}_{,x} + \dot{\phi} w_{,x} + \phi \dot{w}_{,x}\right)^2 \\ & + MI_{zz}\left(\dot{w}_{,x} - \dot{\phi} v_{,x} - \phi \dot{v}_{,x}\right)^2 \\ & + MI_{yz}\left(\dot{v}_{,x} + \phi \dot{w}_{,x} + \phi \dot{w}_{,x}\right)\left(\dot{w}_{,x} - \dot{\phi} v_{,x} - \phi \dot{v}_{,x}\right) \\ & + MI_{zz}\left(\dot{\phi} + \dot{v}_{,x} w_{,x} + v_{,x} \dot{w}_{,x}\right)^2 + MI_{yy}\dot{\phi}^2 \} \, \mathrm{d}x \end{aligned} \tag{6}$$

where m is the mass per unit length of the rod and y_{cg} and z_{cg} the cross-sectional coordinates of the center of mass, defined as follows:

$$y_{cg} = \frac{1}{m} \int\int_A \rho y \, \mathrm{d}A \tag{7a}$$

$$z_{cg} = \frac{1}{m} \int\int_A \rho z \, \mathrm{d}A \tag{7b}$$

The components of the mass moment of inertia per unit length MI_{ij} is given by

$$MI_{yy} = \int\int_A \rho y^2 \, \mathrm{d}A \tag{8a}$$

$$MI_{zz} = \int\int_A \rho z^2 \, \mathrm{d}A \tag{8b}$$

$$MI_{yz} = \int\int_A \rho yz \, \mathrm{d}A \tag{8c}$$

Without any basic problems, it is possible to continue the derivation using the complete expression for the kinetic energy [Eq. (6)]. For many practical applications, however, certain assumptions can be made that result in significant simplifications in the kinetic energy expressions without appreciable degradation in the accuracy results. These assumptions are as follows:

1) y_{cg} and z_{cg} are small enough such that, while their products with quadratic terms of the displacements and lower powers are retained, terms of higher order than quadratic including y_{cg} and z_{cg} may be neglected.

2) The components of the mass moments of inertia are small enough such that their products with terms of order higher than third in the angular displacements are neglected.

As a result of the last assumptions, the expression for the kinetic energy [Eq. (6)] becomes

$$\begin{aligned} T = \frac{1}{2} \int_0^L & \left[m\left(\dot{u}^2 + \dot{v}^2 + \dot{w}^2\right) + 2my_{cg}\dot{w}\dot{\phi} - 2mz_{cg}\dot{v}\dot{\phi} \right. \\ & + MI_{yy}\left(\dot{v}_{,x}^2 + \dot{\phi}^2 + 2\dot{v}_{,x}\dot{\phi} w_{,x} + 2\dot{v}_{,x}\dot{w}_{,x}\phi\right) \\ & + MI_{zz}\left(\dot{w}_{,x}^2 + \dot{\phi}^2 + 2\dot{v}_{,x}\dot{\phi} w_{,x} - 2\dot{v}_{,x}\dot{w}_{,x}\phi\right) \\ & \left. + MI_{yz}\left(\dot{v}_{,x}\dot{w}_{,x} + \dot{w}_{,x}\dot{\phi} w_{,x} + \dot{w}_{,x}^2\phi - \dot{v}_{,x}\dot{\phi} v_{,x} - \dot{v}_{,x}^2\phi\right)\right] \mathrm{d}x \end{aligned} \tag{9}$$

Following the same process applied in Ref. 1 (Eqs. 26 a–c, 36) generalized coordinates are used to describe the elastic displacements:

$$u = \sum_{n=1}^{N_u} q_{u(n)} FU_{(n)} \tag{10a}$$

$$v = \sum_{j=1}^{N_v} q_{v(j)} FV_{(j)} \tag{10b}$$

$$w = \sum_{k=1}^{N_w} q_{w(k)} FW_{(k)} \tag{10c}$$

$$\phi = \sum_{\ell=1}^{N_\phi} q_{\phi(\ell)} F\phi_{(\ell)} \tag{10d}$$

If the rod is assumed to be inextensible (as in Ref. 1), then $q_{u(n)}$ is given by Eq. (39) of Ref. 1. Substituting Eqs. (10) into Eq. (9) and carrying out the spanwise integration yields the following expression for the kinetic energy:

$$\begin{aligned} T = \frac{1}{2} \Bigg\{ & \sum_{j=1}^{N_v} \sum_{j1=1}^{N_v} \left[Q1_{(j,j1)} + Q2_{(j,j1)}\right] \dot{q}_{v(j)} \dot{q}_{v(j1)} \\ & + \sum_{k=1}^{N_w} \sum_{k1=1}^{N_w} \left[Q3_{(k,k1)} + Q4_{(k,k1)}\right] \dot{q}_{w(k)} \dot{q}_{w(k1)} \\ & + \sum_{\ell=1}^{N_\phi} \sum_{\ell 1=1}^{N_\phi} Q5_{(\ell,\ell 1)} \dot{q}_{\phi(\ell)} \dot{q}_{\phi(\ell 1)} + \sum_{j=1}^{N_v} \sum_{k=1}^{N_w} Q6_{(j,k)} \dot{q}_{v(j)} \dot{q}_{w(k)} \\ & + \sum_{j=1}^{N_v} \sum_{\ell=1}^{N_\phi} Q7_{(j,\ell)} \dot{q}_{v(j)} \dot{q}_{\phi(\ell)} + \sum_{k=1}^{N_w} \sum_{\ell=1}^{N_\phi} Q8_{(k,\ell)} \dot{q}_{w(k)} \dot{q}_{\phi(\ell)} \\ & + \sum_{j=1}^{N_v} \sum_{k=1}^{N_w} \sum_{\ell=1}^{N_\phi} \left[Q9_{(j,k,\ell)} \dot{q}_{v(j)} \dot{q}_{\phi(\ell)} q_{w(k)} \right. \\ & \left. + Q10_{(j,k,\ell)} \dot{q}_{v(j)} \dot{q}_{w(k)} q_{\phi(\ell)}\right] + \sum_{j=1}^{N_v} \sum_{j1=1}^{N_v} \sum_{\ell=1}^{N_\phi} Q11_{(j,j1,\ell)} \\ & \times \left[\dot{q}_{v(j)} \dot{q}_{\phi(\ell)} q_{v(j1)} + \dot{q}_{v(j)} \dot{q}_{v(j1)} q_{\phi(\ell)}\right] \sum_{k=1}^{N_w} \sum_{k1=1}^{N_w} \sum_{\ell=1}^{N_\phi} Q12_{(k,k1,\ell)} \\ & \times \left[\dot{q}_{w(k)} \dot{q}_{\phi(\ell)} q_{w(k1)} + \dot{q}_{w(k)} \dot{q}_{w(k1)} q_{\phi(\ell)}\right] \\ & + \sum_{j=1}^{N_v} \sum_{j1=1}^{N_v} \sum_{j2=1}^{N_v} \sum_{j3=1}^{N_v} H11_{(j,j1,j2,j3)} \dot{q}_{v(j)} \dot{q}_{v(j2)} q_{v(j1)} q_{v(j3)} \\ & + \sum_{k=1}^{N_w} \sum_{k1=1}^{N_w} \sum_{k2=1}^{N_w} \sum_{k3=1}^{N_w} H22_{(k,k1,k2,k3)} \dot{q}_{w(k)} \dot{q}_{w(k2)} q_{w(k1)} q_{w(k3)} \\ & + \sum_{j=1}^{N_v} \sum_{j1=1}^{N_v} \sum_{k=1}^{N_w} \sum_{k1=1}^{N_w} H12_{(j,j1,k,k1)} \dot{q}_{v(j)} \dot{q}_{w(k)} q_{v(j1)} q_{w(k1)} \Bigg\} \end{aligned} \tag{11}$$

where

$$H11_{(j,j1,j2,j3)} = 4\sum_{n=1}^{N_u}\sum_{n1=1}^{N_u} Q13_{(n,n1)} H1_{(n,j,j1)} H1_{(n1,j2,j3)} \tag{12a}$$

$$H22_{(k,k1,k2,k3)} = 4\sum_{n=1}^{N_u}\sum_{n1=1}^{N_u} Q13_{(n,n1)} H2_{(n,k,k1)} H2_{(n1,k2,k3)} \tag{12b}$$

$$H12_{(j,j1,k,k1)} = 8\sum_{n=1}^{N_u}\sum_{n1=1}^{N_u} Q13_{(n,n1)} H1_{(n,j,j1)} H2_{(n1,k,k1)} \tag{12c}$$

The integrals $Q1$–$Q13$ are defined in Appendix A. $H1$ and $H2$ are defined by Eqs. (40a) and (40b) of Ref. 1.

The Equations of Motion

The Lagrangian[3] of the system L_g is defined as

$$L_g = T - V \tag{13}$$

where V is the total potential; it has been calculated in Ref. 1 for a rod that is acted on by a distributed conservative load. If Lagrange's equations[3] are applied, then the equations of motion become

$$\frac{d}{dt}\left(\frac{\partial T}{\partial \dot{q}_{v(j)}}\right) - \frac{\partial T}{\partial q_{v(j)}} = -\frac{\partial V}{\partial q_{v(j)}}, \qquad 1 \le j \le N_v \tag{14a}$$

$$\frac{d}{dt}\left(\frac{\partial T}{\partial \dot{q}_{w(k)}}\right) - \frac{\partial T}{\partial q_{w(k)}} = -\frac{\partial V}{\partial q_{w(k)}}, \qquad 1 \le k \le N_w \tag{14b}$$

$$\frac{d}{dt}\left(\frac{\partial T}{\partial \dot{q}_{\phi(\ell)}}\right) - \frac{\partial T}{\partial q_{\phi(\ell)}} = -\frac{\partial V}{\partial q_{\phi(\ell)}}, \qquad 1 \le \ell \le N_\phi \tag{14c}$$

The right-hand sides of Eqs. (14) have been derived in Ref. 1 and those derivations will be used in what follows. If Eq. (10) is substituted into Eqs. (14) and the indicated differentiations performed, the following equations of motion in matrix form are obtained:

$$[[M_1] + [M_2]]\{\ddot{q}\} = -[[K] + [K_2] + [K_3]]\{q\} + \{f_p\} - \{f_s\} + \{f_m\} \tag{15}$$

where $\{q\}$ is the vector of unknowns defined as

$$\{q\}^t = \langle q_{v(1)}, \ldots, q_{v(j)}, \ldots, q_{v(N_v)}; \; q_{w(1)}, \ldots, q_{w(k)}, \ldots, q_{w(N_w)}; \; q_{\phi(1)}, \ldots, q_{\phi(\ell)}, \ldots, q_{\phi(N_\phi)} \rangle \tag{16}$$

The square matrices $[K_1], [K_2], [K_3]$ and the vectors $[f_p]$ and $[f_s]$ are defined in Ref. 1. (The curvature model used is that developed in Appendix A of Ref. 1.) Matrix $[M_1]$ is an assemblage of linear inertia elements, while matrix $[M_2]$ incorporates the nonlinear terms. Vector $\{f_m\}$ can be described as

$$\{f_m\}^t = \langle FMV_{(1)}, \ldots, FMV_{(jm)}, \ldots, FMV_{(Nv)}; \; FMW_{(1)}, \ldots, FMW_{(km)}, \ldots, FMW_{(Nw)}; \; FM\phi_{(1)}, \ldots, FM\phi_{(\ell m)}, \ldots, FM\phi_{(N\phi)} \rangle \tag{17}$$

The elements of $[M_1]$ and $[M_2]$ as well as those in Eq. (17) are defined in Appendix B, the latter by Eqs. (B5).

As regards the solution of these equations, it should be noted that if the displacements and velocities ($\{q\}$ and $\{\dot{q}\}$) at a certain moment are known and the time history of the applied load after this moment is also given, then integration at Eq. (15) will yield the vector $\{q\}$ at any moment afterward.

Small Vibrations Superimposed on Finite Deformations

In this section, the case of small free vibrations superimposed on steady, finite predeformations (e.g., as would result from transverse static loads) is considered. The initial static loading vector is $\{f_p\}_0$ and it results in a generalized displacement vector $\{q\}_0$ that is not a function of time. The equilibrium equation then becomes (see Eq. 15),

$$0 = -([K_1] + [K_2]_0 + [K_3])\{q\}_0 + \{f_p\}_0 - \{f_s\}_0 \tag{18}$$

where, $[K_2]_0$ and $\{f_s\}_0$ are the special forms of $[K_2]$ and $\{f_s\}$, respectively, in which $\{q\}_0$ is substituted for $\{q\}$.

The small, free vibrations are defined by the vector $\{\Delta q\}$, which is a function of time. The resultant generalized displacement vector becomes

$$\{q\} = \{q\}_0 + \{\Delta q\} \tag{19}$$

Substituting Eq. (19) into Eq. (15), neglecting nonlinear terms $\{\Delta q\}$, and using Eq. (18) result in the following equation:

$$([M_1] + [M_2]_0)\{\Delta\ddot{q}\} = -([K_1] + [K_2]_0 + [K_3])\{\Delta q\} - [\Delta K_2]\{q\}_0 - \{\Delta f_s\} \tag{20}$$

The matrix $[M_2]_0$ is obtained by substituting $\{q\}_0$ into Eqs. (B4) of Appendix B. Similarly, $[\Delta K_2]$ is obtained by substituting Eq. (19) into Eq. (28) of Ref. 1, assembling $[K_2]$ according to Eq. (32c) of Ref. 1, and retaining only linear terms in $\{\Delta q\}$. The vector $\{\Delta f_s\}$ is obtained by substituting Eq. (19) into Eq. (51) of Ref. 1 and again retaining only linear terms in $\{\Delta q\}$.

According to the above definition of $[\Delta K_2]$ it is possible to define a new matrix $[K_4]$ such that

$$[\Delta K_2]\{q_0\} = [K_4]_0\{\Delta q\} \tag{21}$$

where the rth column of $[K_4]_0$ is

$$\begin{Bmatrix} K_{4(1,r)} \\ K_{4(2,r)} \\ K_{4(N,r)} \end{Bmatrix} = \left(\frac{\partial}{\partial q_{(r)}}[K_2]\right)_{\{q\}=\{q\}_0} \{q\}_0, \qquad 1 \le r \le N \tag{22}$$

The derivatives of $[K_2]$ with respect to $q_{(\alpha)}$ have been defined in Ref. 1 (the matrices $Q_{(r)}$) and are given by Eqs. (52a) and (52b) of that reference.

The vector $\{\Delta f_s\}$, according to its definition above, can be described as follows:

$$\{\Delta f_s\} = [K_5]_0\{\Delta q\} \tag{23}$$

where the α, β element of $[K_5]_0$ is

$$K_{5(\alpha,\beta)} = \left(\frac{\partial}{\partial q_{(\beta)}} \left(f_{s(\alpha)} \right) \right)_{\{q\}=\{q\}_0} \tag{24}$$

Detailed expressions for $K_{5(\alpha,\beta)}$ are given in Appendix C. Comparison of Eq. (22) with Eq. (C3) reveals that the contribution to $[K_5]$ of the first term on the right side of Eq. (C3) is exactly the transpose of $[K_4]$. Taking advantage of this fact reduces the amount of calculation. Since the contribution of the second term on the right side of Eq. (C5) yields a symmetric matrix, it is clear that the sum $([K_4]_0 + [K_5]_0)$ forms a symmetric matrix. Since we are concerned here only with small, free undamped vibrations, Δq can be expressed as a pure sinusoid in time; i.e.,

$$\{\Delta q\} = \{\mu\} e^{i\omega t} \tag{25}$$

where $\{\mu\}$ is the generalized mode shape and ω the natural angular frequency of that mode.

Substitution of Eqs. (21), (23), and (25) into Eq. (20) yields the final equations of small natural vibrations superimposed on the finite deformations of the rod,

$$\left[[K_0] - \omega^2 [M_0] \right] \{\mu\} = 0 \tag{26}$$

where:

$$[K_0] = [K_1] + [K_2]_0 + [K_3] + [K_4]_0 + [K_5]_0 \tag{27a}$$

$$[M_0] = [M_1] + [M_2]_0 \tag{27b}$$

Thus the solution procedure includes the following steps:

1) The deformation of the rod under the static load $\{q\}_0$ is calculated by the method outlined in Ref. 1.

2) The matrices $[M_2]_0$, $[K_2]_0$, $[K_4]_0$, $[K_5]_0$, and $[M_2]_0$ are assembled as described in the text between Eqs. (20) and (24).

3) The matrices $[K_0]$ and $[M_0]$ are assembled according to Eqs. (27).

4) The eigenvalue problem [Eq. (26)] is solved and the frequencies and mode shapes are obtained.

Results and Discussion

To check the accuracy of the model derived above, the theoretical results are compared in this section with existing experimental and other theoretical results.[4,5]

The case under consideration is shown in Fig. 1. A cantilevered rod is loaded transversely by a tip weight that causes a substantial deformation. Then, the deformed rod is excited in both the flatwise and edgewise directions (z and y, respectively) and the frequencies of the first natural mode in each direction is found. The experiments included changes in the tip weight magnitude and the load angle γ (see Fig. 1). Two aluminum rods with identical rectangular cross sections but different lengths have been used. The rod properties are outlined in Table 1.

In Ref. 2, the value for $EI_{\eta\eta}$ was taken as that which made the theoretically predicted deflection match experiment for one specific load angle. This provided a structural base from which nonlinear effects as influenced by load angle changes could be assessed. It was not possible to determine $EI_{\xi\xi}$ directly from the static experiments, so its value was obtained by dividing $EI_{\eta\eta}$ by 16, based on a cross-sectional width-to-thickness ratio of 4. All the properties used here except for $EI_{\xi\xi}$ are identical to those which were used in Ref. 2 in calculating the static behavior of a similar rod. The value of $EI_{\xi\xi}$ has been changed from the Ref. 2 (2.2668 N · m^2) value in the calculations reported in this paper so as to make the theoretical value of the first flatwise frequency with zero tip weight match the experimental value given in Ref. 4.

Table 1 Rod properties

Principal bending stiffness components	
$EI_{\eta\eta}$	36.2695 N · m^2
$EI_{\xi\xi}$	2.4783 N · m^2
Torsional rigidity GJ	2.9623 N · m^2
Mass per unit length m	0.11317 kg/m
Mass moment of inertia components	
$MI_{\eta\eta}$	$1521.1 \cdot 10^{-9}$ kg · m
$MI_{\xi\xi}$	$95.07 \cdot 10^{-9}$ kg · m
Length	
Rod I	0.508 m (20 in.)
Rod II	0.762 m (30 in.)

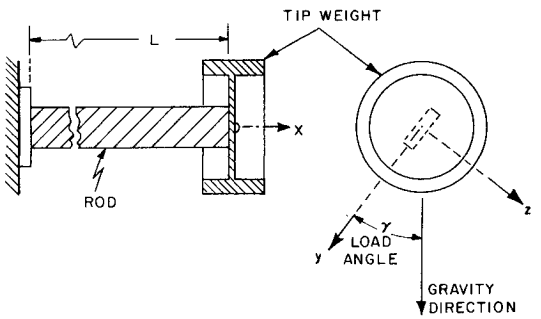

Fig. 1 Rod and tip weight before deformation.

The tip weight is modeled as a concentrated mass and moment of inertia. Mathematically, this is achieved by using the Dirac (impulse) function. Exact analytic expressions exist for the integrals associated with these Dirac functions.

The frequency of the first flatwise mode of rod I is presented in Fig. 2 for three tip weights: 4.448, 8.896, and 13.344 N (1, 2, and 3 lb, respectively), as a function of 0-90 deg load angles ($0 \le \gamma \le 90$ deg). The results of the present theory are compared in this figure with three other sets of results for the same cases: 1) the experimental results of Refs. 4 and 5; 2) results of a linear calculation (where $\{q\}_0$ is taken equal to zero in the present analysis); and 3) the theoretical results presented in Refs. 4 and 5. In all cases, the results of the present theory agree quite well with the test results, showing smaller deviations from the experimental points than the theoretical results of Refs. 4 and 5. The improved predictions clearly are associated with including higher-order terms in the strain expressions, since dropping such terms in the present calculations caused larger discrepancies as compared to the experiments. It is noteworthy, however, that at a tip weight of 8.896 N (2 lb) the trends associated with the theoretical results of Refs. 4 and 5 differ from those given by experiment. No theoretical results from Refs. 4 and 5 are shown in Fig. 2 for the highest load; the static load results for that case appear to predict unbounded values of deformation. The present mathematical model continues to show reasonable trends for all tip weights, even as higher-order terms are dropped. As would be expected, the results of the linear analysis are unaffected by changes in load angle, which is also shown in Fig. 2.

These results show that, at zero load angle, the flatwise frequency is lower than predicted by linear theory. As the load angle is increased, the frequency also increases; at 90 deg, its value is higher than that given by the linear prediction. As would be expected, such nonlinear influences increase as the tip weight and, thus, the static predeformations increase. The percentage increase in the frequency at $\gamma = 90$ deg over the linear result is shown by Fig. 2 to be 2, 6, and 10% for tip weights of 4.448, 8.896, and 13.344 N, respectively. Since this corresponds to predeformation amplitudes of 16, 29, and 40% of beam length, this provides some indication of the measure of the influence of the predeformations on the first flatwise natural frequency.

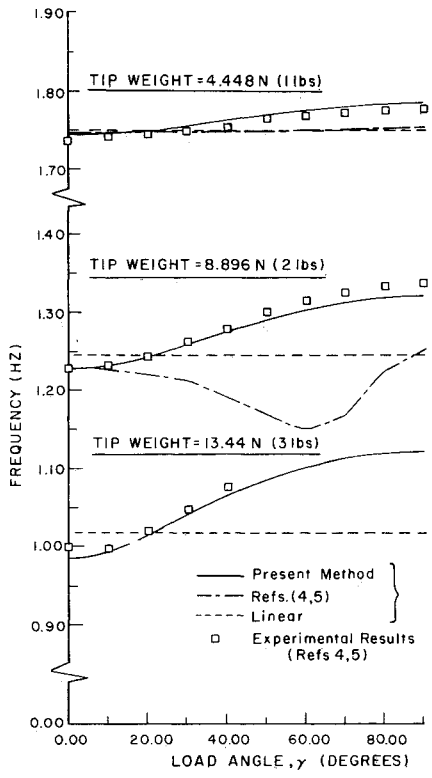

Fig. 2 Rod I: first flatwise natural frequency as a function of load angle and tip weight.

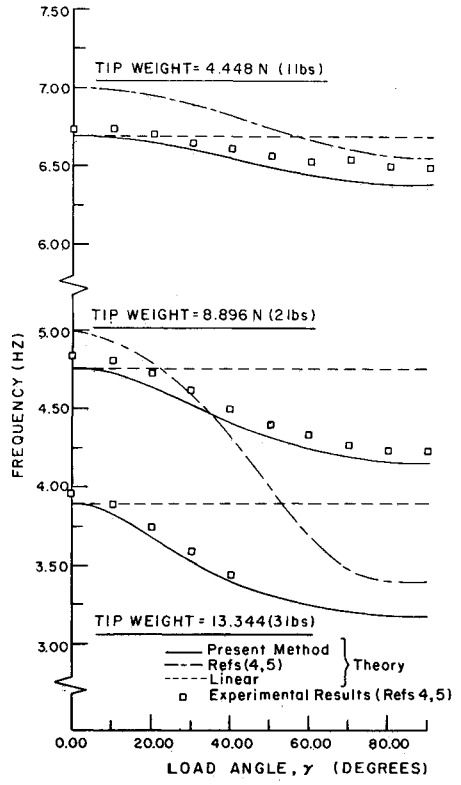

Fig. 3 Rod I: first edgewise natural frequency as a function of load angle and tip weight.

Figure 3 presents for the first edgewise mode, the same comparisons as Fig. 2 for the first flatwise mode. Here again, it can be seen that the agreement between the results of the present theory and experimental results is very good. The influence of the load angle in this case, however, is different from the case of the flatwise mode. At zero load angle, linear and nonlinear analyses give practically identical results. As the load angle increases, the first edgewise frequency decreases. At a load angle of 90 deg and tip load of 4.448 N (1 lb), the reduction in frequency due to nonlinear effects is 5%. Such reductions due to nonlinear effects are 13 and 19% for tip weights of 8.896 and 13.344 N (2 and 3 lb), respectively. In general, it seems that the influences of nonlinear effects on edgewise modes are larger than on flatwise modes.

In Figs. 4 and 5, the first flatwise and edgewise natural frequencies of rod II are presented as functions of the tip weight and load angle and compared with test results from Refs. 4 and 5. The behavior and trends for rod II are similar to those obtained for rod I and the agreement between the results of the present nonlinear theory and experiment is good. Theoretical results were not available for this case from Refs. 4 and 5.

Figure 6 presents the first flatwise frequency for both rods as functions of the tip weight at a load angle of zero degrees ($\gamma = 0$ deg). The predeformation in this case consists only of edgewise displacements v. Both the linear and nonlinear results of the present theory are, again, compared to the experimental results from Refs. 4 and 5. The agreement between experimental and nonlinear theoretical results in this case is also very good. The errors inherent in the linear mathematical model increase, as could be expected, as the tip weight is increased, yielding higher and higher frequency predictions relative to the correct values. The trend of these curves indicates that, at a certain static load level, the first flatwise natural frequency will become zero, thus suggesting a lateral-torsional buckling of the cantilevered rod.[6]

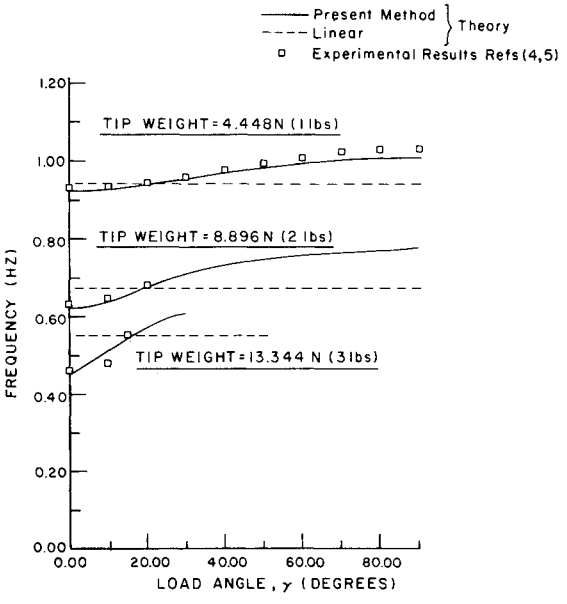

Fig. 4 Rod II: first flatwise natural frequency as a function of load angle and tip weight.

Plots of first natural bending frequencies for rods I and II are given in Fig. 7 for the edgewise case, as they were for the flatwise bending in Fig. 6. In this case, however, the results of linear and nonlinear models are practically identical and show very good agreement with the experimental results.

It is noteworthy that numerical investigations showed that even in these cases, in which a tip mass whose dimensions are relatively large compared to those of the beam cross section is present, but which may be considered concentrated relative to beam length, the influence of mass moments of inertia is very small and may be neglected from a practical point of view in predicting the lowest mode natural frequencies.

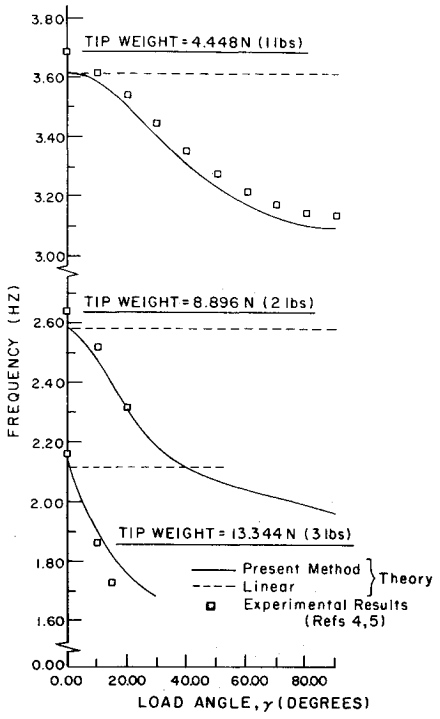

Fig. 5 Rod II: first edgewise natural frequency as a function of load angle and tip weight.

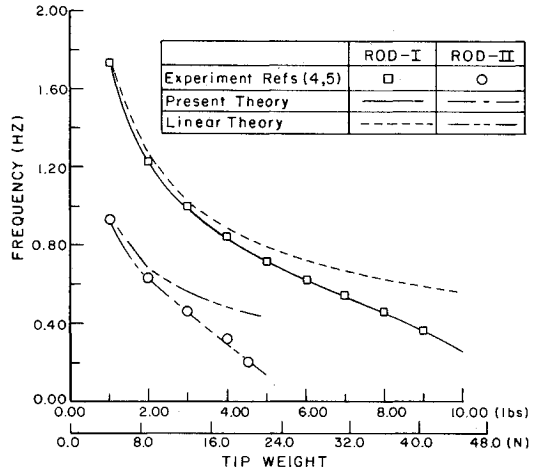

Fig. 6 First flatwise natural frequency as a function of tip weight, at zero load angle ($\gamma = 0$ deg).

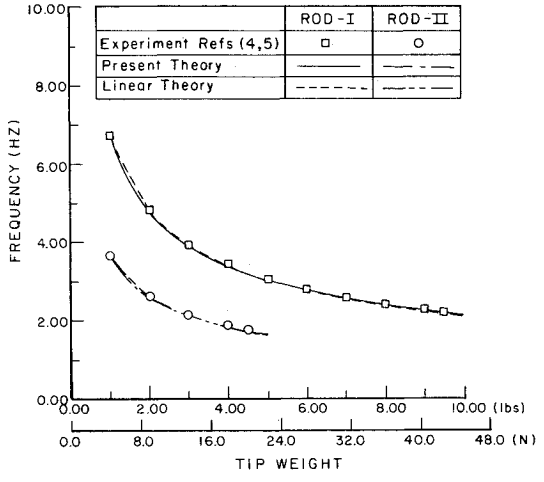

Fig. 7 First edgewise natural frequency as a function of tip weight, at zero load angle ($\gamma = 0$ deg).

Summary and Conclusions

A theory for analyzing the dynamics of a rod undergoing small strains and moderate elastic rotations has been developed. Lagrange equations were used to derive the equations of motion. The addition of a generalized coordinate description for deflections resulted in an efficient mathematical method.

The structural contributions were accounted for by applying a recently developed "principal curvature transformation." This method proved to be accurate and efficient in the nonlinear analysis of rods under static loads.

In deriving the kinetic energy, warping and transverse shear deformations have been neglected, but all slender rod influences were accounted for, including cross-sectional mass center offset and mass moments of inertia. After area integration for these properties, however, products of the cross-sectional mass moments of inertia with certain higher-order terms, as well as products of center of mass offset with certain other higher-order terms were neglected. While these assumptions significantly decreased the manipulations required in the derivations, all those terms could be retained if necessary. A derivation identical in principle to the one presented, but much more tedious in the number of terms carried, would lead to the final and complete equations.

A perturbation of the equations of motion yielded the system of equations governing the small vibrations of a rod deformed by an initial, steady load. Solving this eigenvalue problem yielded the natural frequencies and mode shapes of those vibrations.

The theory has been validated by applying it to cases for which experimental results are available. Very good agreement was obtained. As expected, nonlinear effects increase as the magnitude of predeformations increase. There are different trends in the influence of nonlinear effects for flatwise or edgewise modes. The influence of apparantly substantial mass moment of inertia on the frequencies of the lowest modes appears to be insignificant. Although beyond the scope of this paper, the current theory inherently seems to contain the basis for coupled bending-torsion buckling, as evidenced by the reduction of the first flatwise frequency toward zero as the magnitude of the steady static load increases.

Appendix A

The generalized components of the mass matrix are defined as

$$Q1_{(j,j1)} = \int_0^L mFV_{(j)}FV_{(j1)}\,dx \tag{A1}$$

$$Q2_{(j,j1)} = \int_0^L MI_{yy}FV'_{(j)}FV'_{(j1)}\,dx \tag{A2}$$

$$Q3_{(k,k1)} = \int_0^L mFW_{(k)}FW_{(k1)}\,dx \tag{A3}$$

$$Q4_{(k,k1)} = \int_0^L MI_{zz}FW'_{(k)}FW'_{(k1)}\,dx \tag{A4}$$

$$Q5_{(\ell,\ell1)} = \int_0^L (MI_{yy} + MI_{zz})F\phi_{(\ell)}F\phi_{(\ell1)}\,dx \tag{A5}$$

$$Q6_{(j,k)} = \int_0^L MI_{yz}FV'_{(j)}FW'_{(k)}\,dx \tag{A6}$$

$$Q7_{(j,\ell)} = -2\int_0^L mZ_{cg}FV_{(j)}F\phi_{(\ell)}\,dx \tag{A7}$$

$$Q8_{(k,\ell)} = 2\int_0^L my_{cg}FW_{(k)}F\phi_{(\ell)}\,dx \tag{A8}$$

$$Q9_{(j,k,\ell)} = 2\int_0^L (MI_{yy} + MI_{zz})FV'_{(j)}FW'_{(k)}F\phi_{(\ell)}\,dx \tag{A9}$$

$$Q10_{(j,k,\ell)} = 2\int_0^L (MI_{yy} - MI_{zz})FV'_{(j)}FW'_{(k)}F\phi_{(\ell)}\,dx \tag{A10}$$

$$Q11_{j(j,j1,\ell)} = -\int_0^L MI_{yz} FV'_{(j)} FV'_{(j1)} F\phi_{(\ell)}\, dx \tag{A11}$$

$$Q12_{(k,k1,\ell)} = \int_0^L MI_{yz} FW'_{(k)} FW'_{(k1)} F\phi_{(\ell)}\, dx \tag{A12}$$

$$Q13_{(n,n1)} = \int_0^L mFU_{(n)} FU_{(n1)}\, dx \tag{A13}$$

where:

$$1 \le j, \qquad j1 \le N_v \tag{A14}$$

$$1 \le k, \qquad k1 \le N_w \tag{A15}$$

$$1 \le \ell, \qquad \ell 1 \le N_\phi \tag{A16}$$

Appendix B: Matrices $[M_1]$, $[M_2]$ and Vector $\{f_m\}$

The linear matrix $[M_1]$ is an assembly of the following submatrices:

$$[M_1] = \begin{bmatrix} [LM1] & [LM2] & [LM3] \\ [LM4] & [LM5] & [LM6] \\ [LM7] & [LM8] & [LM9] \end{bmatrix} \tag{B1}$$

where

$[LM1]$ is an $N_v \times N_v$ matrix with elements

$$LM1_{(jm,j)} = Q1_{(jm,j)} + Q2_{(jm,j)} \tag{B2a}$$

$[LN2]$ is an $N_v \times N_w$ matrix with elements

$$LM2_{(jm,k)} = Q6_{(jm,k)}/2 \tag{B2b}$$

$[LM3]$ is an $N_v \times N_\phi$ matrix with elements

$$LM3_{(jm,\ell)} = Q7_{(jm,\ell)}/2 \tag{B2c}$$

$[LM4]$ is an $N_w \times N_v$ matrix with elements

$$LM4_{(km,j)} = Q6_{(j,km)}/2 \tag{B2d}$$

$[Lm5]$ is an $N_w \times N_w$ matrix with elements

$$LM5_{(km,k)} = Q3_{(km,k)} + Q4_{(km,k)} \tag{B2e}$$

$[LM6]$ is an $N_w \times N_\phi$ matrix with elements

$$LM6_{(km,\ell)} = Q8_{(km,\ell)}/2 \tag{B2f}$$

$[LM7]$ is an $N_\phi \times N_v$ matrix with elements

$$LM7_{(\ell m,j)} = Q7_{(j,\ell m)}/2 \tag{B2g}$$

$[LM8]$ is an $N_\phi \times N_w$ matrix with elements

$$LM8_{(\ell m,k)} = Q8_{(k,\ell m)}/2 \tag{B2h}$$

$[LM9]$ is an $N_\phi \times N_\phi$ matrix with elements

$$LM9_{(\ell m,\ell)} = Q5_{(\ell m,\ell)} \tag{B2i}$$

The matrix $[M_2]$ is a nonlinear inertia matrix which is an assembly of the following submatrices:

$$[M_2] = \begin{bmatrix} [NM1] & [NM2] & [NM3] \\ [NM4] & [NM5] & [NM6] \\ [NM7] & [NM8] & [NM9] \end{bmatrix} \tag{B3}$$

where:

$[NM1]$ is an $N_v \times N_v$ matrix with elements

$$NM1_{(jm,j)} = \sum_{\ell=1}^{N_\phi} Q11_{(jm,j,\ell)} q_{\phi(\ell)} + \sum_{j1=1}^{N_v} \sum_{j2=1}^{N_v} H11_{(jm,j,k,k1)} q_{v(j1)} q_{v(j2)} \tag{B4a}$$

$[NM2]$ is an $N_v \times N_w$ matrix with elements

$$NM2_{(jm,k)} = \frac{1}{2}\left[\sum_{\ell=1}^{N_\phi} Q10_{(jm,k,\ell)} q_{\phi(\ell)} + \sum_{j=1}^{N_v} \sum_{k1=1}^{N_w} H12_{(jm,j,k,k1)} q_{v(j1)} q_{w(k1)} \right] \tag{B4b}$$

$[NM3]$ is an $N_v \times N_\phi$ matrix with elements

$$NM3_{(jm,\ell)} = \frac{1}{2}\left[\sum_{j=1}^{N_v} Q11_{(jm,j,\ell)} q_{v(j)} + \sum_{k=1}^{N_w} Q9_{(jm,k,\ell)} q_{w(k)} \right] \tag{B4c}$$

$[NM4]$ is an $N_w \times N_v$ matrix with elements

$$NM4_{(km,j)} = \frac{1}{2} \sum_{\ell=1}^{N_\phi} Q10_{(j,km,\ell)} q_{\phi(\ell)} + \frac{1}{2} \sum_{j1=1}^{N_v} \sum_{k=1}^{N_w} H12_{(j,j1,km,k)} q_{v(j1)} q_{w(k)} \tag{B4d}$$

$[NM5]$ is an $N_w \times N_w$ matrix with elements

$$NM5_{(km,k)} = \sum_{\ell=1}^{N_w} Q12_{(km,k,\ell)} q_{\phi(\ell)} + \sum_{k1=1}^{N_w} \sum_{k2=1}^{N_w} H22_{(km,k1,k,k2)} q_{w(k1)} q_{w(k2)} \tag{B4e}$$

$[NM6]$ is an $N_w \times N_\phi$ matrix with elements

$$NM6_{(km,\ell)} = \frac{1}{2} \sum_{k=1}^{N_w} Q12_{(km,k,\ell)} q_{w(k)} \tag{B4f}$$

$[NM7]$ is an $N_\phi \times N_v$ matrix with elements

$$NM7_{(\ell m,j)} = \frac{1}{2}\left[\sum_{j1=1}^{N_v} Q11_{(j,j1,\ell m)} q_{v(j1)} + \sum_{k=1}^{N_v} Q9_{(j,k,\ell m)} q_{w(k)} \right] \tag{B4g}$$

$[NM8]$ is an $N_\phi \times N_w$ matrix with elements

$$NM8_{(\ell m,k)} = \frac{1}{2} \sum_{k1=1}^{N_w} Q12_{(k,k1,\ell m)} q_{w(k1)} \tag{B4h}$$

$[NM9]$ is a zero $N_\phi \times N_\phi$ matrix.

The elements of the vector $\{f_m\}$ (Eq. 17) are defined as follows:

$$FMV_{(jm)} = \frac{1}{2}\sum_{k=1}^{N_w+N_\phi}\sum_{\ell=1}\left[Q9_{(jm,k,\ell)} + Q10_{(jm,k,\ell)}\right]\dot{q}_{w(k)}\dot{q}_{\phi(\ell)} + \sum_{j=1}^{N_v}\sum_{\ell=1}^{N_\phi} Q11_{(jm,j,\ell)}\dot{q}_{v(j)}\dot{q}_{\phi(\ell)} + \frac{1}{2}\sum_{j=1}^{N_v}\sum_{k=1}^{N_w}\sum_{k1=1}^{N_w} H12_{(jm,j,k,k1)}\dot{q}_{w(k)}\dot{q}_{w(k1)}q_{v(j)} \quad \text{(B5a)}$$

$$FMW_{(km)} = \frac{1}{2}\sum_{j=1}^{N_v}\sum_{\ell=1}^{N_\phi}\left[Q10_{(j,km,\ell)} - Q9_{(j,km,\ell)}\right]\dot{q}_{v(j)}\dot{q}_{\phi(\ell)} + \sum_{k=1}^{N_v}\sum_{\ell=1}^{N_\phi} Q12_{(km,k,\ell)}\dot{q}_{w(k)}\dot{q}_{\phi(\ell)} + \frac{1}{2}\sum_{j=1}^{N_v}\sum_{j1=1}^{N_v}\sum_{k=1}^{N_w} H12_{(j,j1,km,k)}\dot{q}_{v(j)}\dot{q}_{v(j1)}q_{w(k)} \quad \text{(B5b)}$$

$$FM\phi_{(\ell m)} = \frac{1}{2}\sum_{j=1}^{N_v}\sum_{k=1}^{N_w}\left[Q9_{(j,k,\ell m)} - Q10_{(j,k\ell m)}\right]\dot{q}_{v(j)}\dot{q}_{w(k)} \quad \text{(B5c)}$$

Appendix C: Matrix $[K_5]_0$

According to Eqs. (51) and (52a) of Ref. 1, $f_{s(r)}$ is defined as follows:

$$f_{s(r)} = \tfrac{1}{2}\{q\}^t\left[Q_{(r)}\right]\{q\} \qquad 1 \le r \le N_v + N_w + N_\phi \quad \text{(C1)}$$

where:

$$\left[Q_{(r)}\right] = \left[DD3_{(r)}\right]^t[D4][D2] + [D2]^t[D4]\left[DD3_{(r)}\right] + \left[DD3_{(r)}\right]^t[D4][D3] + [D3]^t[D4]\left[DD3_{(r)}\right] \quad \text{(C2)}$$

On the right side of Eq. (C2), only the matrix $[DD3_{(r)}]$ is a function of $\{q\}$.

Substitution of Eq. (C1) into Eq. (24), using the symmetry of $[Q_{(r)}]$ as defined by Eq. (C2), yields

$$K_{5(\alpha,\rho)} = \{q\}_0^t\left[Q_{(\alpha)}\right]_{\{q\}=\{q\}_0}\{\mu_{(\beta)}\} + \tfrac{1}{2}\{q\}_0^t\left[Q_{(\alpha,\beta)}\right]_{\{q\}=\{q_0\}}\{q\}_0 \quad \text{(C3)}$$

where $\{\mu_{(\beta)}\}$ is an N-dimensional vector. The βth element of this vector is equal to unity, while all of the other terms are equal to zero. The matrix $[Q_{(\alpha,\beta)}]$ is formed from the derivative of the matrix $[Q_{(\alpha)}]$ with respect to $q_{(\beta)}$. Differentiation of Eq. (C2) yields:

$$\left[Q_{(\alpha,\beta)}\right] = \left[DE3_{(\alpha,\beta)}\right]^t[D4][D2] + [D2]^t[D4]\left[DE3_{(\alpha,\beta)}\right] + \left[DE3_{(\alpha,\beta)}\right]^t[D4][D3] + [D3]^t[D4]\left[DE3_{(\alpha,\beta)}\right] \quad \text{(C4)}$$

where $[DE3_{(\alpha,\beta)}]$ is an $N_e \times N$ matrix defined as

$$\left[DE3_{(\alpha,\beta)}\right] = \left[\frac{\partial}{\partial q_{(\beta)}}\left[DD3_{(\alpha)}\right]\right]_{\{q\}=\{q\}_0} \quad \text{(C5)}$$

Using the results of Appendices B and C of Ref. 7 [in particular, Eqs. (C22)–(C30)], one obtains

1) $1 \le \alpha \le N_v$; $1 \le \beta \le N_v$

$$\left[DE3_{(\alpha,\beta)}\right] = \begin{bmatrix}[D13VV] & 0 & 0\\ [D15VV] & 0 & 0\\ 0 & 0 & 0\end{bmatrix} \quad \text{(C6)}$$

in which $[D13VV]$ is a $N_{ve} \times N_v$ matrix whose elements are

$$D13VV_{(jm,j)} = 2G22_{(jm,j,\beta,\alpha)} \quad \text{(C7)}$$

and $[D15VV]$ is a $N_{we} \times N_v$ matrix whose elements are

$$D15VV_{(km,j)} = 2G25_{(km,j,\beta,\alpha)} \quad \text{(C8)}$$

2) $1 \le \alpha \le N_v$; $N_v < \beta \le N_v + N_w + N_\phi$

$$\left[DE3_{(\alpha,\beta)}\right] = [0] \quad \text{(C9)}$$

3) $N_v < \alpha \le N_v + N_w$; $1 \le \beta \le N_v$ or $N_v + N_w < \beta \le N_v + N_w + N_\phi$

$$\left[DE3_{(\alpha,\beta)}\right] = [0] \quad \text{(C10)}$$

4) $N_v < \alpha \le N_v + N_w$; $N_v < \beta \le N_v + N_w$

$$S = \alpha - N_v; \quad f = \beta - N_v \quad \text{(C11)}$$

$$\left[DE3_{(\alpha,\beta)}\right] = \begin{bmatrix}[D13WW] & [D14WW] & 0\\ [D13WW] & [D14WW] & 0\\ 0 & 0 & 0\end{bmatrix} \quad \text{(C12)}$$

in which $[D13WW]$ is a $N_{ve} \times N_v$ matrix whose elements are

$$D13WW_{(jm,j)} = G23_{(jm,j,s,f)} + G23_{(jm,j,f,s)} \quad \text{(C13)}$$

$[D14WW]$ is a $N_{ve} \times N_w$ matrix whose elements are

$$D14WW_{(jm,k)}2G24_{(jm,k,f,s)} \quad \text{(C14)}$$

$[D15WW]$ is a $N_{we} \times N_v$ matrix whose elements are

$$D15WW_{(km,j)} = G26_{(km,j,f,s)} + G26_{(km,j,s,f)} \quad \text{(C15)}$$

and $[D16WW]$ is a $N_{we} \times N_w$ matrix whose elements are

$$D16WW_{(km,k)} = 2G27_{(km,k,f,s)} \quad \text{(C16)}$$

5) $N_v + N_w < \alpha \le N_v + N_w + N_\phi$

$$\left[DE3_{(\alpha,\beta)}\right] = 0 \quad \text{(C17)}$$

References

[1]Rosen, A., Loewy, R.G., and Mathew, M.B., "Nonlinear Analysis of Pretwisted Rods Using 'Principal Curvature Transformations'—Part I: Theoretical Derivation," *AIAA Journal*, Vol. 25, March 1987, pp. 470–478.

[2]Rosen, A., Loewy, R.G., and Mathew, M.B., "Nonlinear Analysis of Pretwisted Rods Using 'Principal Curvature Transformation'—Part II: Numerical Results," *AIAA Journal*, Vol. 25, April 1987, pp. 598–604.

[3]Washizu, K., *Variational Methods in Elasticity and Plasticity*, Pergamon Press, London, 1968, pp. 104–107.

[4]Dowell, E.H. and Traybar, J., "An Experimental Study of the Non-Linear Stiffness of a Rotor Blade Undergoing Flap, Lag and Twist Deformations," AMS Rept. 1194, Princeton University, Princeton, NJ, Jan. 1975.

[5]Dowell, E.H., Traybar, J., and Hodges, D.H., "An Experimental-Theoretical Correlation Study of Non-Linear Bending and Torsion Deformation of a Cantilever Beam," *Journal of Sound and Vibration*, Vol. 50, No. 4, 1977, pp. 533–544.

[6]Rosen, A., Loewy, R.G., and Mathew, M.B., "Elastic Stability, of Pretwisted Rods," Rensselaer Polytechnic Institute, Troy, NY, RTC Rept. S-85-2, 1985.

[7]Rosen, A., Loewy, R.G., and Mathew, M.B., "A Method of Principal Curvature Transformation for Analysing the Nonlinear Coupled Bending-Torsion of Pretwisted Rods, Part I: Theoretical Derivation," Rensselaer Polytechnic Institute, Troy, NY, RTC Rept. D-85-2, Sept. 1985.